Journal of Pharmaceutical Analysis 2013;3(3):200–204

Contents lists available at ScienceDirect

Journal of Pharmaceutical Analysis

www.elsevier.com/locate/jpa
www.sciencedirect.com

ORIGINAL ARTICLE

Fluorescence spectroscopy of osthole binding to human serum albumin

Guang-De Yang[a], Cong Li[a], Ai-Guo Zeng[a], Yuan Zhao[b], Rong Yang[a], Xiao-Li Bian[a,*]

[a]*School of Medicine, Xi'an Jiaotong University, No. 76 Yanta Westroad, Shaanxi Province, Xi'an 710061, PR China*
[b]*Xi'an Tuberculosis and Thoracic Tumor Hospital, Shaanxi 710061, PR China*

Received 22 June 2012; accepted 13 October 2012
Available online 23 October 2012

KEYWORDS

Osthole;
Human serum albumin;
Fluorescence quenching

Abstract The interaction of human serum albumin (HSA) with osthole was investigated by fluorescence spectroscopy. Osthole can quench the fluorescence of HSA and the quenching mechanism is a static process. The binding site number n and apparent binding constant K were measured at different temperatures. The thermodynamic parameters ΔH^0, ΔG^0 and ΔS^0 were calculated at different temperatures. The results indicated that electrostatic forces played a major role in the interaction of osthole with HSA. Results of osthole synchronous fluorescence and UV absorption spectra showed that the microenvironment and conformation of HSA were changed.

1. Introduction

Human serum albumin (HSA) is the most abundant protein constituent of blood plasma and serves as a protein storage component. It plays an important role in the transport and disposition of endogenous and exogenous ligands in the blood [1].

Strong binding interactions can decrease the concentrations of free drugs in plasma, whereas weak interactions can lead to a short lifetime or poor distribution. Consequently, investigation of the binding interaction between drugs and serum albumin is important in pharmacology and pharmacodynamics.

The binding interaction of drugs to serum albumin *in vitro* has been considered as a model in protein chemistry to study the binding behavior of proteins [2]. In the present study, HSA was selected as our protein model because of its low cost, ready availability, and unusual ligand-binding properties and the results of all of the studies are consistent with the fact that bovine and human serum albumins are homologous proteins [3].

Osthole ($C_{15}H_{16}O_3$, CAS 484-12-8) is a natural coumarin isolated from the fruit of *Cnidium monnieri* (L.) Cusson (Chinese herbal name of Shechuangzi), a Chinese herb widely

*Corresponding author. Tel./fax: +86 29 82657833.
E-mail address: bianxl@mail.xjtu.edu.cn (X.-L. Bian).
Peer review under responsibility of Xi'an Jiaotong University.

Production and hosting by Elsevier

2095-1779 © 2013 Xian Jiaotong University. Production and hosting by Elsevier B.V. All rights reserved.
http://dx.doi.org/10.1016/j.jpha.2012.10.002

used as a remedy for skin disease and gynecopathy [4]. Osthole also exerts pharmacological effects on experimental autoimmune encephalomyelitis [5], epilepsy [6], focal cerebral ischemia [7], and chronic hypoperfusion-induced injury [8]. However, there is very little known about the mode of interaction of osthole with HSA. The quality analytical articles on the active components in traditional Chinese medicine are more [9,10], but research articles on the base are less.

UV and fluorescence absorption spectroscopies are powerful tools for the study of the reactivity of chemical and biological systems [11,12]. The aim of this work was to determine the binding of osthole to HSA under physiological conditions utilizing the fluorescence method, and to investigate the thermodynamics of its interaction.

2. Experimental

2.1. Materials

Osthole (batch number 110822-200305) was purchased from the National Institute for the Control of Pharmaceutical and Bioproducts (Beijing, China). Chemical structure of osthole is shown in Fig. 1. HSA (fatty acid free) fraction V (Cat No. A8230) was purchased from Sigma Chemical Co. (St. Louis, MO, USA). All HSA solutions were prepared in pH 7.40 buffer and stored in dark at 4 °C. A 0.5 M NaCl solution was used to maintain the ion strength. The buffer (pH 7.40) consisted of 0.05 M Tris and 0.1 M HCl. All reagents were of analytical reagent grade and distilled water was used throughout the experiments.

2.2. Instruments

Fluorescence spectra and synchronous fluorescence investigations were carried out on an RF-5301PC fluorophotometer (Shimadzu, Kyoto, Japan). The emission spectra were recorded from 300 to 450 nm (excitation wavelength 278 nm). Synchronous fluorescence spectra of HSA in the absence and presence of increasing amounts of osthole were recorded. All experiments were performed at three temperatures (298, 303 and 310 K). The sample temperature was maintained by recycling water from a super-thermostatic water tank (SYC-15) throughout the experiments. A UV-2450 UV–vis spectrometer (Shimadzu) was used for scanning the UV spectrum.

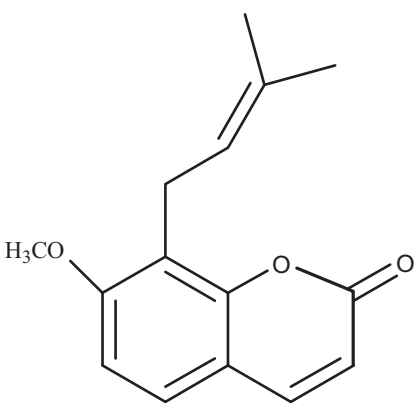

Fig. 1 Chemical structure of osthole.

All pH measurements were made with a PHS-29A digital pH meter (Shanghai Lei Ci Device Works, Shanghai, China) with a combinational glass calomel electrode.

2.3. Spectroscopic measurements

The UV absorption spectra of HSA, osthole and their mixture were measured at room temperature. The fluorescence measurements were performed at different temperatures (298, 303 and 310 K). Excitation wavelength was 278 nm. The excitation and emission slit widths were set at 2.0 nm. Appropriate blanks corresponding to the buffer were subtracted to correct background fluorescence.

2.4. Preparation of stock solution

HSA was dissolved in Tris–HCl buffer solution (0.05 M Tris, 0.5 M NaCl, pH 7.40) to 10^{-5} M. The stock solution of osthole (5.158×10^{-3} M) was prepared by dissolving the drug in double distilled water containing 30% ethanol (osthole is insoluble in water, but soluble in ethanol–water mixture).

3. Results and discussion

3.1. UV characteristics of HSA

To explore the structural changes in HSA by addition of osthole, we measured UV spectra (Fig. 2) of HSA with various amounts of osthole. Fig. 2 shows that the absorption peaks (278 nm) of these solutions had moderate shifts toward the red wavelengths, indicating the addition of osthole. The appearance of the red-shift was indicative of the hydrophobic decrease.

3.2. Fluorescence characteristics of HSA

Concentration of HSA was stabilized at 10^{-5} M, and the content of osthole varied from 0 to 18.2×10^{-9} M. The effects of osthole on HSA fluorescence intensity are shown in Fig. 3.

The intensity of fluorescence can be decreased by a wide variety of processes. Such decreases in intensity are called

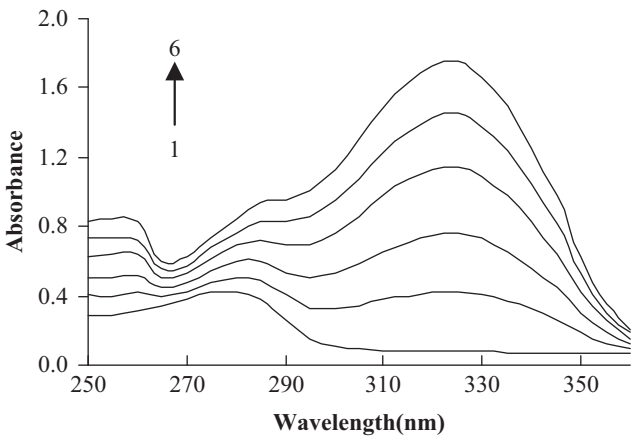

Fig. 2 UV spectra of HSA at different contents of osthole $C_{HSA} = 10^{-5}$ M; $C_{NaCl} = 0.5$ M. 1–6: $C_{osthole} = 0$, 2.6×10^{-8}, 5.2×10^{-8}, 7.8×10^{-8}, 10.4×10^{-8}, 13.0×10^{-8} M.

quenching. It is apparent from Fig. 3 that the fluorescence intensity of HSA decreased regularly with increasing osthole concentration.

Different mechanisms of quenching are usually classified as dynamic and static quenching. Dynamic and static quenching can be distinguished by their differing dependence on temperature and viscosity. The dynamic quenching constants are expected to increase with increasing temperature. In contrast, increasing the temperature is likely to result in decreasing stability of complexes, and thus lowers the static quenching constants [13].

The fluorescence quenching data are usually analyzed by the Stern–Volmer equation [14]

$$\frac{F_0}{F} = 1 + K_q\tau_0[Q] = 1 + K_{SV}[Q] \quad (1)$$

where F_0 and F are the fluorescence intensities before and after addition of quencher (osthole), respectively. K_q is the bimolecular quenching constant, τ_0 is the lifetime of the fluorophore in the absence of quencher, K_{SV} is the Stern–Volmer quenching constant, and $[Q]$ is the concentration of quencher. Hence, Eq. (1) was applied to determine K_{SV} by linear regression of a plot of F_0/F against $[Q]$.

The Stern–Volmer quenching constant K_{SV} of HSA by osthole at different temperatures is shown in Table 1.

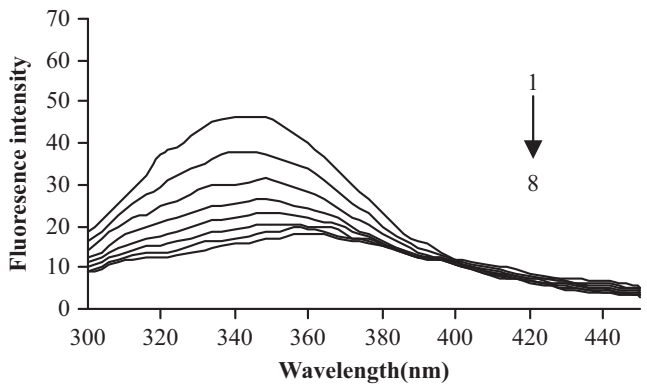

Fig. 3 Emission spectra of HSA in the presence of various concentrations of osthole. $C_{HSA}=10^{-5}$ M; $C_{NaCl}=0.5$ M. 1–8: $C_{osthole}=0$, 2.6×10^{-9}, 5.2×10^{-9}, 7.8×10^{-9}, 10.4×10^{-9}, 13.0×10^{-9}, 15.6×10^{-9}, 18.2×10^{-9} M.

These results indicate that the probable quenching mechanism of fluorescence of HSA by osthole is a static quenching procedure, because K_{SV} decreased with rising temperature.

Consequently, the static quenching data were analyzed according to the Lineweaver–Burk [15,16] and the modified Stern–Volmer equations [13,17]

$$\frac{F_0}{F_0-F} = \frac{K_d}{f_a[Q]} + \frac{1}{f_a} \quad (2)$$

where F_0 and F are the fluorescence intensities before and after addition of quencher (osthole), respectively, f_a is the fraction of accessible fluorescence, K_d is dissociation constant, and $[Q]$ is the concentration of quencher. Hence, Eq. (2) was applied to determine K_d by linear regression of a plot of $F_0/(F_0-F)$ against $1/[Q]$.

The Lineweaver–Burk quenching constant K_d of HSA by osthole at different temperatures is shown in Table 2.

3.3. *Effect of drug on HSA conformation*

The conformational changes of HSA were evaluated by measuring the synchronous fluorescence intensity of protein amino acid residues, before and after the addition of osthole.

When $\Delta\lambda$ between excitation and emission wavelengths is stabilized at 15 or 60 nm, then the synchronous fluorescence gives the characteristic information about tyrosine or tryptophan residues. When $\Delta\lambda=15$ nm, the spectrum characteristic of protein tyrosine residues was observed, and when $\Delta\lambda=60$ nm, the spectrum characteristic of protein tryptophan residues was observed [18].

The concentration of HSA was stabilized at 10^{-5} M, and the concentration of osthole was increased by titration. Synchronous fluorescence spectra of HSA with varying the concentration of osthole were scanned at $\Delta\lambda=15$ or 60 nm (Fig. 4A and B, respectively).

It is apparent from Fig. 4A that the maximum emission wavelength moderately shifts (from 303 to 299 nm) towards blue wavelengths when $\Delta\lambda=15$ nm. The shift effect showed that the conformation of HSA had changed. The blue-shift effect indicated that the microenvironment around the tyrosine residue was disturbed and the hydrophobicity of the residue decreased in the presence of osthole, yet the microenvironment around the tryptophan residues had no discernable change from the binding process [19,20].

Table 1 Stern–Volmer quenching constant K_{SV} and linear equations of osthole–HSA at pH 7.40.

Compound	T (K)	Linear equations	K_{SV} (M^{-1})
Osthole	298	$y=98123x+0.9949$ $R^2=0.9995$	9.812×10^4
	303	$y=96664x+1.0204$ $R^2=0.9997$	9.666×10^4
	310	$y=94038x+1.284$ $R^2=0.9987$	9.404×10^4

Table 2 Lineweaver–Burk quenching constant K_d of the system of quencher HSA.

Compound	T (K)	Linear equations	K_d (M)
Osthole	298	$y=0.992\times10^{-5}x+1.0405$ $R^2=0.9975$	0.953×10^{-5}
	303	$y=1.008\times10^{-5}x+0.9936$ $R^2=0.9997$	1.014×10^{-5}
	310	$y=1.026\times10^{-5}x+0.9932$ $R^2=0.9990$	1.033×10^{-5}

3.4. Analysis of binding equilibria

When small molecules bind independently to a set of equivalent sites on a macromolecule, the equilibrium between free and bound molecules is given by the following equation [13]

$$\lg\left(\frac{F_0-F}{F}\right) = \lg K + n \lg[Q] \quad (3)$$

where in the present case, K is the binding constant to a site, and n is the number of binding sites per HSA molecule. The binding parameters of HSA by osthole at different temperatures are shown in Table 3.

3.5. Interaction force between drug and HSA

Generally, small molecules are bound to macromolecules through four binding modes: hydrogen bonds, van der Waals forces, and electrostatic and hydrophobic interactions [21]. The thermodynamic parameters, enthalpy (ΔH) and entropy (ΔS) of reaction are important for confirming the acting force. The temperatures chosen were 298, 303 and 310 K so that HSA did not undergo any structural degradation. The thermodynamic parameters can be determined from the van't Hoff equation

$$\ln K = \frac{-\Delta H^0}{RT} + \frac{\Delta S^0}{R} \quad (4)$$

$$\Delta G^0 = \Delta H^0 - T\ \Delta S^0 \quad (5)$$

where K is the binding constant at the temperature T and R is the gas constant. The values of ΔH^0 and ΔS^0 are calculated from the slope and intercept of the van't Hoff plot of ln K against $1/T$. The Gibbs energy change ΔG^0 is estimated according to Eq. (5). The thermodynamic parameters at the three temperatures (298, 303 and 309 K) were determined and are presented in Table 4. Ross and Subramanian [22] have characterized the sign and magnitude of the thermodynamic parameters associated with various individual interactions that may take place in protein association processes, as described below. Generally, a positive ΔH value is usually taken as typical evidence for hydrophobic interactions. Furthermore, specific electrostatic interactions between ionic species in aqueous solution are characterized by a positive value of ΔS and a negative ΔH value, whereas negative ΔH value and negative ΔS value changes arise from van der Waals forces and hydrogen bond formation in low dielectric media.

From Table 4, the negative sign for Gibbs energy (ΔG^0) means that the interaction process was spontaneous and the negative ΔH^0 and positive ΔS^0 values indicated that electrostatic forces played major roles in the interaction of osthole with HSA and that the reaction was mainly enthalpy driven.

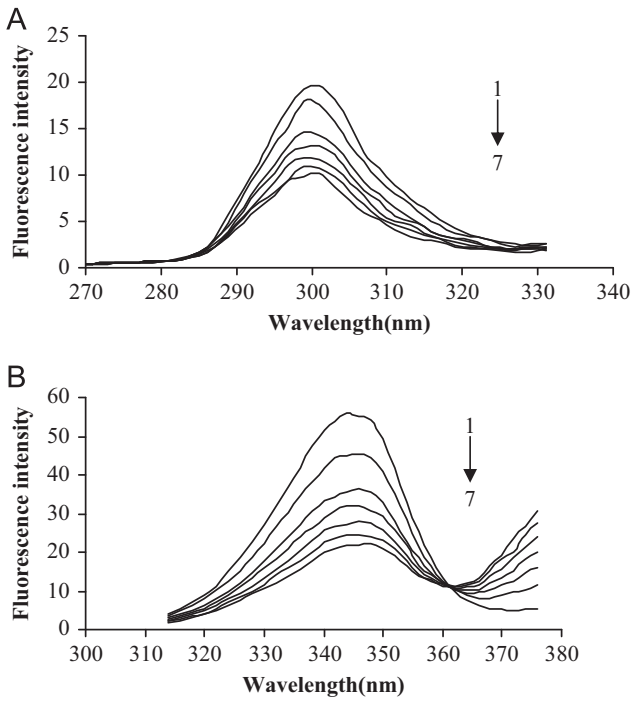

Fig. 4 Synchronous fluorescence spectra of HSA with varying the concentration of osthole: (A) $\Delta\lambda = 15$ nm and (B) $\Delta\lambda = 60$ nm. $C_{HSA} = 10^{-5}$ M; $C_{NaCl} = 0.5$ M. 1–7: $C_{osthole} = 0$, 2.6×10^{-9}, 5.2×10^{-9}, 7.8×10^{-9}, 10.4×10^{-9}, 13.0×10^{-9}, 15.6×10^{-9} M.

4. Conclusions

In this study, the interaction of osthole with HSA was studied by spectroscopic methods, including fluorescence and UV absorption spectroscopy. Our results clearly indicate that osthole is a strong quencher. The Stern–Volmer quenching constant and corresponding thermodynamic parameters ΔH^0, ΔG^0 and ΔS^0 were calculated. The thermodynamic parameter calculations show that, for osthole, the acting forces were mainly electrostatic, which played the major role in the interaction of osthole with HSA. Synchronous fluorescence

Table 4 Thermodynamic parameters for the quenching of osthole–HSA at three different temperatures.

Compound	T (K)	ΔG^0 (kJ/mol)	ΔH^0 (kJ/mol)	ΔS^0 (J/K mol)
Osthole	298	−28.3056	−9.519	63.041
	303	−28.6208		
	310	−29.0621		

Table 3 Binding parameters of osthole–HSA at three different temperatures.

Compound	T (K)	Linear equations	K (M^{-1})	n
Osthole	298	$y = 0.9958x + 4.9681$ $R^2 = 0.9986$	9.298×10^4	0.99
	303	$y = 0.9875x + 4.9332$ $R^2 = 0.9997$	8.574×10^4	0.99
	310	$y = 0.9819x + 4.8972$ $R^2 = 0.9985$	4.944×10^4	0.98

spectra showed that the microenvironment and conformation of HSA were changed in the presence of osthole.

Acknowledgments

This project was supported by the National Natural Science Foundation of China (Grant nos. 30873194 and 21172177) and Natural Science Foundation of Shaanxi Province (2012K14-05-03).

References

[1] X.M. He, D.C. Carter, Atomic structure and chemistry of human serum albumin, Nature 358 (186) (1992) 209–215.
[2] Y.J. Hu, Y. Liu, X.S. Shen, et al., Studies on the interaction between 1-hexylcarbamo 5-fluorouracil and bovine serum albumin, J. Mol. Struct. 738 (1–3) (2005) 143–147.
[3] J. Guharay, B. Sengupta, P.K. Sengupta, Protein–flavonol interaction: fluorescence spectroscopic study, Proteins 43 (2) (2001) 75–81.
[4] Q.S. Lian, Progress in study of chemical constituents and pharmacological effects of the fruits of *Cnidium monnieri*, Chin. Med. Mater. 26 (2) (2003) 141–144.
[5] X. Chen, R. Pi, Y. Zou, et al., Attenuation of experimental autoimmune encephalomyelitis in C57 BL/6 mice by osthole, a natural coumarin, Eur. J. Pharmacol. 629 (1–3) (2010) 40–46.
[6] J.J. Luszczki, E. Wojda, M. Andres-Mach, et al., Anticonvulsant and acute neurotoxic effects of imperatorin, osthole and valproate in the maximal electroshock seizure and chimney tests in mice: a comparative study, Epilepsy Res. 85 (2–3) (2009) 293–299.
[7] W. He, J.X. Liu, Y.M. Zhou, et al., Protective effects of Osthole on cerebral ischemia–reperfusion injury in rats and its mechanism, Chin. Pharmacol. Bull. 24 (11) (2008) 1528–1530.
[8] H.J. Ji, J.F. Hu, Y.H. Wang, et al., Osthole improves chronic cerebral hypoperfusion induced cognitive deficits and neuronal damage in hippocampus, Eur. J. Pharmacol. 636 (1–3) (2010) 96–101.
[9] M. Li, X.F. Hou, J. Zhang, et al., Applications of HPLC/MS in the analysis of traditional Chinese medicines, J. Pharm. Anal. 1 (2) (2011) 81–91.
[10] X.F. Chen, H.T. Wu, G.G. Tan, et al., Liquid chromatography coupled with time-of-flight and ion trap mass spectrometry for qualitative analysis of herbal medicines, J. Pharm. Anal. 1 (4) (2011) 235–245.
[11] J. Zhang, H.H. Sun, Y.Z. Zhang, et al., Interaction of human serum albumin with indomethacin: spectroscopic and molecular modeling studies, J. Solution Chem. 41 (3) (2012) 422–443.
[12] Y. Li, W. He, J. Liu, et al., Binding of the bioactive component Jatrorrh izine to human serum albumin, Biochim. Biophys. Acta 1722 (1) (2005) 15–21.
[13] S.S. Lehrer, Solute perturbation of protein fluorescence. Quenching of the tryptophyl fluorescence of model compounds and of lysozyme by iodide ion, Biochemistry 10 (17) (1971) 3254–3263.
[14] J.R. Lakowicz, in: Principles of Fluorescence Spectroscopy, second ed., Plenum Press, New York, 1999.
[15] S. Deepa, A.K. Mishra, Fluorescence spectroscopic study of serum albumin bromadiolone interaction: fluorimetric determination of bromadiolone., J. Pharm. Biomed. Anal. 38 (3) (2005) 556–563.
[16] N. Barbero, E. Barni, C. Barolo, et al., A study of the interaction between fluorescein sodium salt and bovine serum albumin by steady-state fluorescence, Dyes Pigm. 80 (3) (2009) 307–313.
[17] Y.Z. Zhang, B. Zhou, Y.X. Liu, et al., Fluorescence study on the interaction of bovine serum albumin with p-aminoazobenzene, J. Fluoresc. 18 (1) (2008) 109–118.
[18] J.N. Miller, Recent advances in molecular luminescence analysis, Proc. Anal. Div. Chem. Soc. 16 (3) (1979) 203–208.
[19] Y.J. Hu, W. Li, Y. Liu, et al., Fluorometric investigation of the interaction between methylene blue and human serum albumin, J. Pharm. Biomed. Anal. 39 (3-4) (2005) 740–745.
[20] S.Y. Cui, X.L. Hu, J.Q. Liu, Study of the binding of herbacetin to bovine serum albumin by fluorescence spectroscopy, J. Solution Chem. 40 (5) (2011) 764–774.
[21] C.Q. Jiang, M.X. Gao, X.Z. Meng, Study of the interaction between daunorubicin and human serum albumin, and the determination of daunorubicin in blood serum samples, Spectrochim. Acta A: Mol. Biomol. Spectrosc. 59 (7) (2003) 1605–1610.
[22] P.D. Ross, S. Subramanian, Thermodynamics of protein association reaction: forces contribution to stability, Biochemistry 20 (11) (1981) 3096–3102.